available at www.sciencedirect.com

ScienceDirect

journal homepage: www.elsevier.com/locate/biochempharm

# Volume-activated chloride channels contribute to cell-cycle-dependent regulation of HeLa cell migration

*Jianwen Mao* [a,**], *Lixin Chen* [b], *Bin Xu* [a], *Lijing Wang* [a], *Weizhang Wang* [a], *Ming Li* [a], *Min Zheng* [a], *Hongzhi Li* [a], *Jiao Guo* [a], *Weidong Li* [a], *Tim J.C. Jacob* [d], *Liwei Wang* [c,*]

[a] *Institute of Basic Medical Sciences and Department of Biology, Guangdong Pharmaceutical University, Guangzhou Higher Education Mega Center, Guangzhou, Guangdong, 510006, China*
[b] *Department of Pharmacology, Medical College, Jinan University, Guangzhou, Guangdong, 510632, China*
[c] *Department of Physiology, Medical College, Jinan University, Guangzhou, Guangdong, 510632, China*
[d] *Cardiff School of Biosciences, Cardiff University, Cardiff CF10 3US, UK*

ARTICLE INFO

*Article history:*
Received 28 July 2008
Accepted 2 October 2008

*Keywords:*
Chloride channels
Cell cycle
Cell migration
ClC-3
Antisense oligonucleotide

ABSTRACT

The activation of volume-activated chloride $Cl^-$ channels has been implicated to play important roles in modulating cell cycle and cell migration. The aim of this study was to determine whether volume-activated $Cl^-$ channels are involved in cell-cycle-dependent regulation of cell migration in HeLa cells. Using techniques including cell-cycle synchronization, transwell migration assays and the patch-clamp technique, we demonstrate in this study that both the expression of volume-activated chloride current ($I_{Cl,vol}$) and the potential of cell migration are cell-cycle-dependent; specifically, these events were high in $G_0/G_1$ phase, low in S phase, and medium in $G_2/M$ phase. Moreover, the mean density of $I_{Cl,vol}$ was positively correlated to the rate of cell migration during cell-cycle progression. Additionally, endogenous suppression of $I_{Cl,vol}$ by transfecting cells with ClC-3 antisense oligonucleotides arrested cells in S phase and slowed cell migration. Collectively, our results suggest that volume-activated $Cl^-$ channels contribute to the cell-cycle-dependent regulation of cell migration.



## 1. Introduction

Tumor growth occurs as a result of aberrant cell-cycle regulation. However, metastasis needs not only aberrant cell-cycle regulation, but also increased motility of malignant cells. Studies have evidenced the relationship between migratory activity of cells and their position in the cell cycle [1]. In fact, some mammalian cell lines demonstrate decreased motility in the $G_2$ phase when compared to that in the $G_1$/S phase [2]. Specifically, concanavalin A-induced lymphocyte migration was lower for cells in late S and $G_2/M$ compared to cells in $G_0/G_1$ and early S phases [3]. Furthermore, p27 and p21, two cell-cycle regulators, are also known to be involved in regulating cell migration [4–6].

Volume-activated chloride current ($I_{Cl,vol}$), with its characteristic biophysical and pharmacological properties, is critical for the regulatory volume decrease (RVD) process after cell swelling [7,8]. $I_{Cl,vol}$ has also been implicated to have important roles in modulating cell-cycle progression [9], although controversy exists regarding the relationship between $I_{Cl,vol}$ and

* *Corresponding author*. Tel.: +86 20 85220260.
** *Corresponding author*. Tel.: +86 20 39352126.
E-mail addresses: wangliweic@sohu.com (L. Wang), jianwenmao@hotmail.com (J. Mao).
0006-2952/$ – see front matter 
doi:10.1016/j.bcp.2008.10.009

cell-cycle progression. For example, in mouse fibroblasts, the magnitude of $I_{Cl,vol}$ was similar in S phase compared to $G_0/G_1$ [10]. However, in SiHa human cervical cancer cells, the $I_{Cl,vol}$ was down-regulated in $G_0/G_1$ and increased in S [11]. In contrast, in Ehrlich Lettre Ascites (ELA) cells, $I_{Cl,vol}$ decreased in $G_1$ and increased in early S phase, when compared to that in $G_0$ [12]. Our previous results showed that in nasopharyngeal carcinoma CNE-2Z cells, expression of $I_{Cl,vol}$ was high in $G_1$ phase, down-regulated in S phase, and again increased in M phase [13].

Volume-sensitive $Cl^-$ channels are also involved in many other physiological cell activities that are associated with changes in cell volume and shape [14]. In glioma cells, for example, inhibition of swelling-activated $Cl^-$ channels inhibits tumor cell migration with these particular $Cl^-$ channels localized to lipid-raft domains on invadipodia [15–17]. Consistent with this, our previous work demonstrated that pharmacological inhibition of $I_{Cl,vol}$ inhibits CNE-2Z cell migration [18], and that $I_{Cl,vol}$ regulates CNE-2Z cell migration by modulating RVD [19,20]. However, it is unclear whether $I_{Cl,vol}$ is involved in cell-cycle-related changes of cell migration. The aim of this study is to investigate the role of volume-sensitive $Cl^-$ channels in cell-cycle-dependent regulation of cell migration in HeLa cells.

## 2. Materials and methods

### 2.1. Cell preparation

HeLa cells from epithelioid carcinoma of human cervix were routinely seeded at a density of $1.3 \times 10^4/cm^2$ and grown in 25-$cm^2$ plastic tissue culture flasks in RPMI 1640 medium with 10% fetal calf serum (FCS), 100 IU/mL penicillin and 100 μg/mL streptomycin at 37 °C in a humidified atmosphere of 5% $CO_2$. Cells were subcultured every 2 days. For electrophysiological experiments, cells that had been cultured for 48 h and reached 80% confluency were trypsinized and resuspended in culture medium. This cell suspension was plated onto round coverslips of 22-mm diameter (150 μL/coverslip) and incubated at 37 °C for approximately 2–3 h before current recordings were taken.

### 2.2. Cell synchronization

Cell-cycle synchronization of HeLa cells was achieved by three well-established methods. First, after exponentially growing cells were treated for 12 h with 0.25 μM demecolcine. The "mitotic shake-off" (also termed "mitotic detachment") method, which can provide highly synchronous cultures of mitotic cells [21,22], was used to collect mitotically enriched floating cells from adherent cells. Second, the double-block technique [21] was used to synchronize cells in S phase. For this, cells were incubated in 2 mM thymidine for 14 h, then in normal medium for 10 h and finally in hydroxyurea (2 mM) for 14 h. Cells were harvested and cultured in normal medium for 4 h to release cells from block. The third method involved serum deprivation, which synchronized cells in $G_0/G_1$ phase. Cells at 60–70% confluence were incubated in RPMI 1640 medium with 0.2% FCS for 48 h. Cell-cycle distribution of control and synchronized cultures were determined by a FACScan flow cytometer (Becton Dickinson, San Jose, CA). Data were acquired with Cell Quest software, and the percentage of $G_0/G_1$, S and $G_2$/M phase cells was calculated with MODFIT software (Verity Software House, Inc., Topsham, ME).

### 2.3. Electrophysiological studies

Whole-cell currents of single HeLa cells were recorded using the patch-clamp technique with a List EPC-7 patch-clamp amplifier (List Electronic, Darmstadt, Germany). Experiments were carried out at room temperature (20–24 °C). The patch-clamp pipettes were made from standard wall borosilicate glass capillaries with an inner filament on a two-stage vertical puller and gave a resistance of 4–6 MΩ when filled with pipette solution. Cell capacitance compensation and series resistance compensation were used to minimize voltage errors. The amplifier reading of capacitance was used as the value for whole-cell membrane capacitance. Once the whole-cell configuration was established, cells were held at the chloride equilibrium potential (0 mV) and then stepped repeatedly to 200 ms pulses of 0, ±40 and ±80 mV, with 4 s intervals between steps. Command voltages and whole-cell currents were recorded simultaneously on a computer via a laboratory interface (CED 1401, Cambridge, UK) with a sampling rate of 3 kHz. The voltage pulse generation, data collection and current analysis were performed using EPC software (CED, Cambridge, UK). All current measurements were collected at 10 ms following the onset of each voltage step.

### 2.4. Transwell migration assay

A modified version of a transwell migration technique described previously [18] was used. Briefly, $3 \times 10^5$ HeLa cells (100 μL) were added to 12 μm-pore transwell inserts, which had been coated with 10 μL fibronectin (FN, 1 mg/mL) and air-dried, and placed into wells of a 24-well plate. All assays were performed at 37 °C in 5% $CO_2$ and humidified air for 6 h. Cells that migrated and attached to the lower surface of the filter were trypsinized and resuspended in 300 μL RPMI 1640 medium. This cell suspension was added to the upper compartment of a new transwell insert not precoated with FN. Next, both inserts (including non-migrated and migrated cells) were placed into another 24-well tissue culture plate with each well containing 600 μL medium and 100 μL MTT (5 mg/mL). Four hours after re-incubation, inserts were put on filter paper and the medium was blotted. Subsequently, 100 μL DMSO was added to solubilize the formazan. Finally, the color solution was transferred to a separate well in a 96-well culture plate, and the absorbance was colorimetrically measured at 570 nm. The percentage of migrated cells (migration rate) was calculated with the OD values of non-migrated and migrated cells. The rate of migration = $OD_{mig}/(OD_{mig} + OD_{non}) \times 100\%$, where $OD_{mig}$ is the OD value of migrated cells and $OD_{non}$ is the OD value of non-migrated cells.

### 2.5. Western blot analysis

For protein extraction, HeLa cells were first washed with PBS once, and the whole-cell lysate was next prepared using lysis buffer containing Tris–Cl (50 mM), NaCl (150 mM), $NaN_3$

(0.02%), Nonidet P-40 (1%), SDS (0.1%), sodium deoxycholate (0.5%), leupeptin (5 μg/mL), and aprotinin (1 μg/mL). Protein content of cell lysates was quantified with Coomassie Brilliant Blue. Proteins of interest were separated by SDS-PAGE and transferred to nitrocellulose membranes (Schleicher & Schuell, Keene, NH), and membranes were blocked at room temperature (24–26 °C) for 1 h in a solution containing (in mM): 130 NaCl, 2.5 KCl, 10 $Na_2HPO_4$, and 1.5 $KH_2PO_4$, and 0.1% Tween 20 and 5% BSA (pH 7.4). Membranes were next incubated first with a polyclonal antibody directed against ClC-3 ($C_{670–687}$) (a gift from Dr. William J. Hatton [23]) overnight at 4 °C and then with a peroxidase-conjugated antibody (HRP-linked anti-rabbit secondary antibody) for 1 h at room temperature. Final detection was accomplished with Western blot luminol reagent (SC-2048; Santa Cruz Biotechnology Inc., California, USA) as described by the manufacturer. The density of target bands was quantified by the computer-aided 1D gel analysis system.

### 2.6. Treatments with antisense and sense oligonucleotides

Antisense and sense oligonucleotides corresponding specifically to the initiation codon region of human ClC-3 mRNA were synthesized (Sangon, Shanghai, China) as reported in our previous study [24]. The antisense sequence was 5′-TCCATTTGTCATTGT-3′; for sense, the sequence was 5′-ACAATGACAAATGGA-3′. For the two oligonucleotides, the first three bases at either end were phosphorothioated. To examine uptake of these constructs by HeLa cells, oligonucleotides were labeled with fluorescence. The identity and purity of oligonucleotides were confirmed by [$^{31}$P]-NMR, capillary gel electrophoresis, hybridization melting temperature and the $A_{269}$/mass ratio. All oligonucleotides had purities higher than 95% with a phosphodiester content lower than 0.3%. Cells were transfected with oligonucleotides in the presence of lipofectamine 2000 (5 μL/mL, Invitrogen, CA, USA) in serum-free medium for 4.5 h and then in medium containing 10% fetal calf serum for additional time depending on the experiment being performed.

### 2.7. Solutions and chemicals

The pipette solution contained (in mM): 70 *N*-methyl-D-glucamine chloride (NMDG-Cl), 10 HEPES, 1.2 $MgCl_2$, 1 EGTA, 140 D-mannitol, and 2 ATP. The isotonic bath solution contained (in mM): 70 NaCl, 0.5 $MgCl_2$, 2 $CaCl_2$, 10 HEPES, and 140 D-mannitol. The 47% hypotonic bath solution was obtained by omitting D-mannitol from the solution, giving an osmolarity of 160 mosmol/L (47% hypotonicity compared to the isotonic solution). The 47% hypertonic solution was obtained by adding D-mannitol to the isotonic solution, giving an osmolarity of 440 mosmol/L (47% hypertonicity, compared to the isotonic solution). The pH of the pipette and bath solutions was adjusted to 7.25 and 7.4, respectively, with Tris base. 5-Nitro-2-(3-phenylpropylamino)benzoic acid (NPPB) and tamoxifen were dissolved with dimethyl sulfoxide (DMSO) and methanol, respectively, resulting in a concentration of 100 mM. Solutions were diluted to their final concentrations for each experiment using corresponding solutions. All chemicals in the study were purchased from Sigma (St. Louis, MO, USA).

### 2.8. Statistics

Data are expressed as mean ± standard error (number of observations). ANOVA was used to analyze data to detect statistically significant differences and Student Newman–Keuls was employed as the post hoc identifying test. $P < 0.05$ indicated significant difference. All experiments were repeated at least 3 times. The $IC_{50}$, the inhibition concentration at which the inhibition is 50%, was obtained by curve fitting on the data obtained with the different concentrations of inhibitors using a four parameter logistic equation, $y = y_0 + (a - y_0)/(1 + (x/x_0)b)$. The parameters $x$ and $y$ are the concentration of the given reagent and the response value (inhibition), $a$ and $y_0$ the maximum and minimum inhibition, $x_0$ and $b$ the $x$ value at the maximum rate of change and the slope coefficient, respectively.

## 3. Results

### 3.1. Volume-activated $Cl^-$ currents in HeLa cells

We hypothesize that $Cl^-$ currents are activated during both cell-cycle progression and migration of HeLa cells, since these events require the cell to undergo shape and volume changes. Volume-activated $Cl^-$ channels may be involved in cell progression and migration. To first examine the properties of volume-activated $Cl^-$ currents in unsynchronized HeLa cells, unsynchronized HeLa cells were voltage clamped at 0 mV in the whole-cell configuration and stepped repeatedly to 0, ±40, and ±80 mV. As shown in Fig. 1A and B, under the isotonic condition, these cells possessed a small and stable current of 6.90 ± 1.67 pA/pF at +80 mV and −5.15 ± 1.43 pA/pF at −80 mV ($n$ = 18). When changed to a 47% hypotonic solution, the current was increased, at ±80 mV, to 80.69 ± 5.95 and −44.87 ± 4.52 pA/pF ($n$ = 18), respectively. The currents were outward rectified and lacked time-dependent inactivation at the voltages tested. The increase in current was partially reversible upon return to isotonic conditions in 10 min. Extending the bathing period in isotonic conditions after the hypotonic challenge would return further the swelling-activated current towards normal level, but 30–60 min was needed to fully return the cells to normal. The residual swelling-activated current could also be eliminated by perfusing cells with hypertonic (47%) solution. Addition of the chloride channel blocker NPPB (300 μM) into the hypertonic solution speeded up the hypertonic effect on the residual current. The cells appeared swollen under hypotonic conditions and remained so until subjected to isotonic conditions. The swelling-activated current exhibited an almost linear current–voltage ($I$–$V$) relationship (Fig. 1B). In experiments ($n$ = 18) with nearly identical $Cl^-$ concentrations inside and outside of the cells, the reversal potential of the $I$–$V$ curve was close to the calculated $E_{Cl}$ (−0.9 mV), with a mean value of −2.5 ± 1.2 mV.

Currents activated by hypotonic challenge were almost completely inhibited by external application of two well known $Cl^-$ channel blockers, NPPB (300 μM) and tamoxifen (20 μM). Fig. 1C–F shows current traces of representative cells exposed to hypotonicity, the effect of adding NPPB or

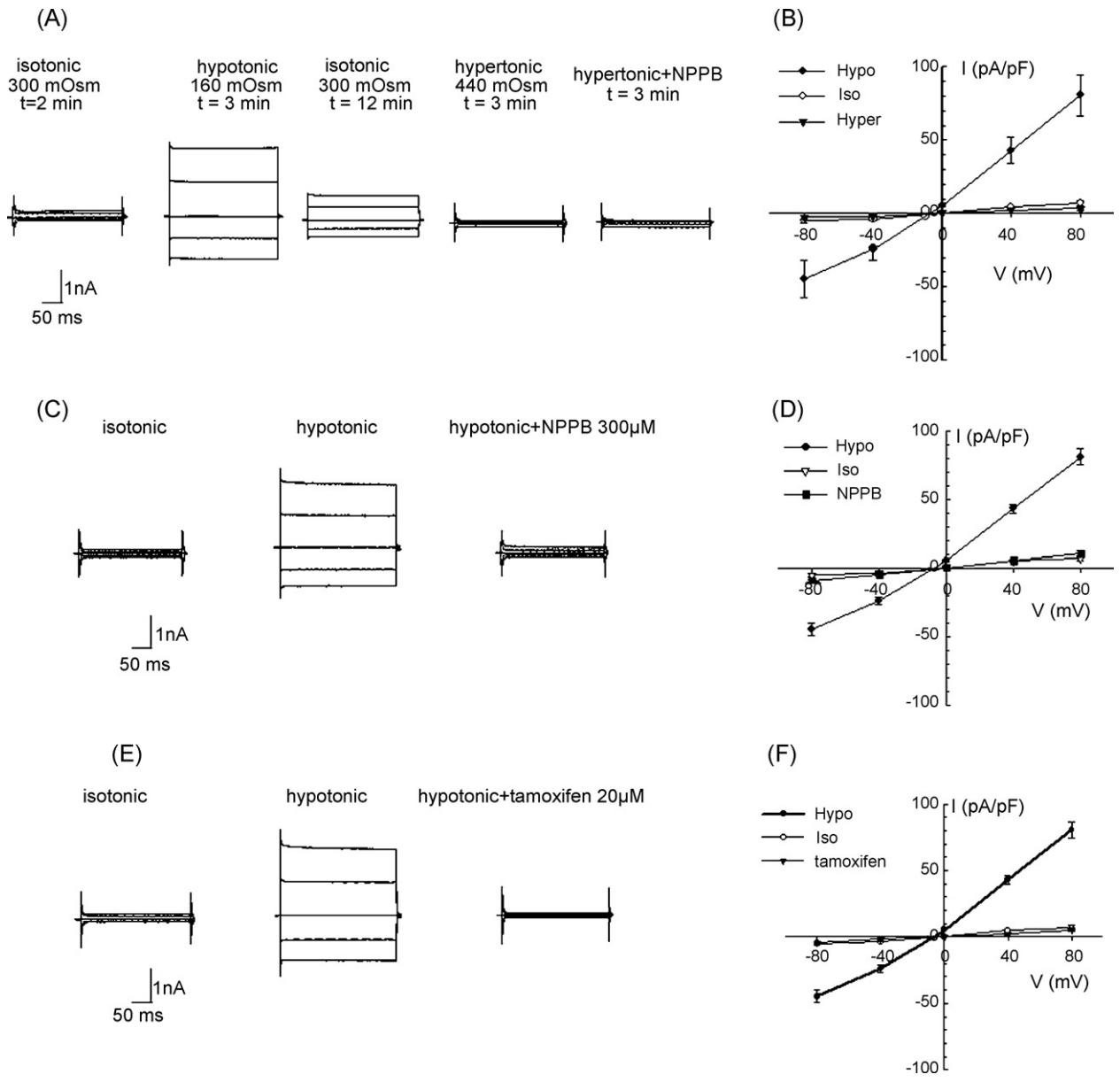


**Fig. 1 – Volume-activated $Cl^-$ current in HeLa cells. (A) Current traces recorded under isotonic conditions and at the peak of 47% hypotonic conditions, upon return to isotonic, in 47% hypertonic bath solution and in 47% hypertonic bath solution plus chloride channel blocker NPPB (300 μM) in response to 0, ±40, ±80 voltage steps. (B) The current–voltage (*I–V*) relationship is presented (*n* = 18). (C) and (E) show typical current traces recorded under isotonic and 47% hypotonic conditions and the effects of extracellular application of NPPB (300 μM) and tamoxifen (20 μM) on the hypotonic-activated current. (D and F) *I–V* relationship under different conditions (*n* = 5). Iso, isotonic bath solution; Hypo, 47% hypotonic bath solution; Hyper, 47% hypertonic bath solution. The time in (A) shows the time period exposed in the indicated condition.**

tamoxifen, and the corresponding *I–V* relationship ($n = 5$ independent experiments). The inhibitory effects were reversible and concentration-dependent. Fitting the data with the four parameter logistic equation (see Section 2), gave an $IC_{50}$ of 178.13 μM for NPPB and 9.34 μM for tamoxifen.

### 3.2. *Cell synchronization*

To investigate expression of volume-sensitive currents and the migration ability at different stages of the cell cycle, HeLa cells were synchronized by serum starvation, chemical block, or by combining mitotic shake-off with demecolcine treatments as described in Section 2. As demonstrated by flow cytometry, highly synchronized cells were obtained (Fig. 2A and D). In unsynchronized cells, 57.5%, 25.7%, and 16.8% of the population were distributed in $G_0/G_1$, S and $G_2/M$ phases, respectively. Cells were sampled at 48 h following incubation in medium containing 0.2% fetal calf serum. At this point, 82% of the cells were in $G_0/G_1$ phases. When cells were treated with combined application of thymidine and hydroxyurea, 88% of

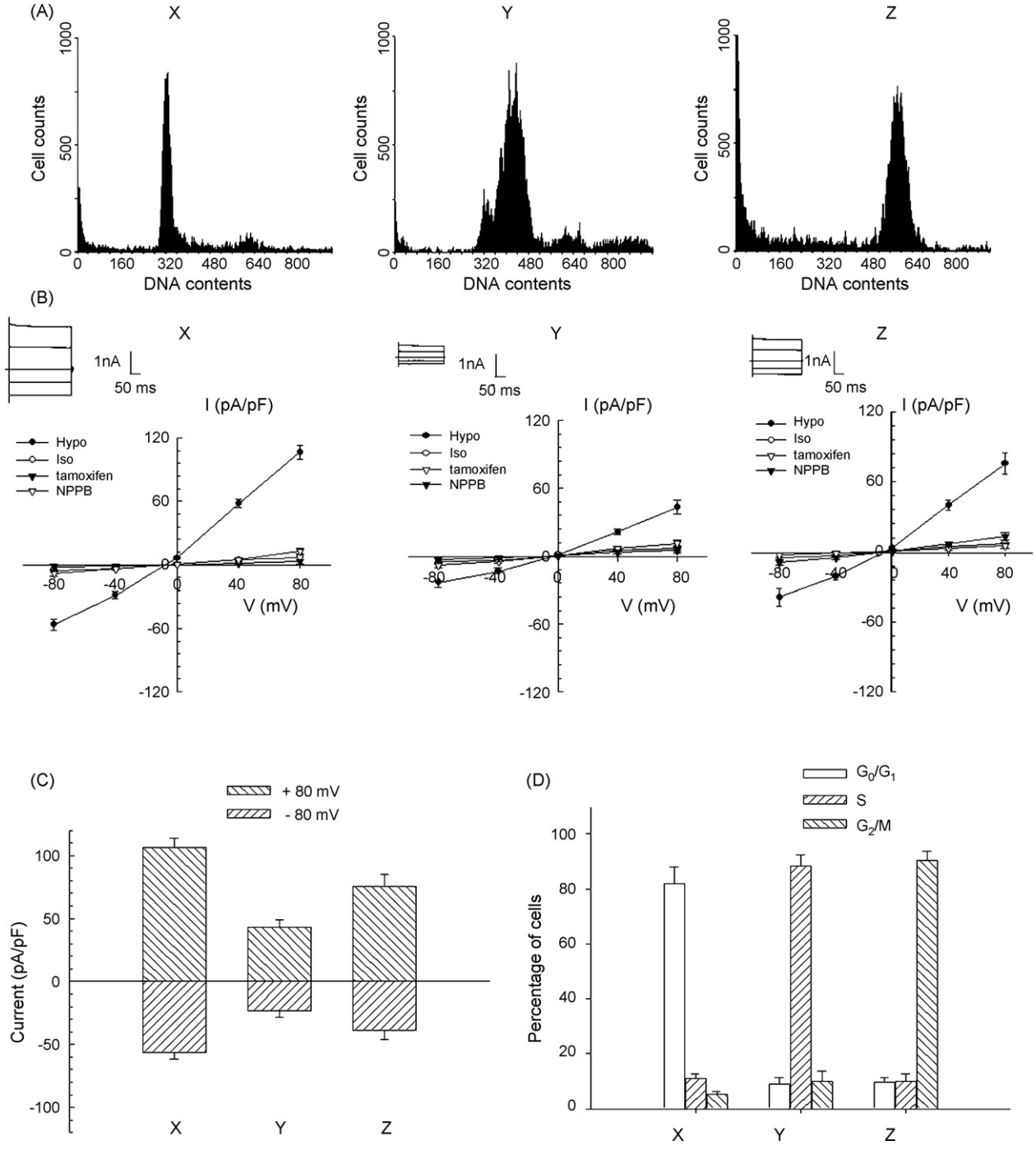


**Fig. 2 – Cell-cycle-dependent expression of volume-activated $Cl^-$ current. Cells were arrested at different phases of the cell cycle by three methods: X, cells incubated in the medium with 0.2% fetal calf serum for 48 h ($G_0/G_1$ phases); Y, cells treated with 2 mM thymidine and 2 mM hydroxyurea (S phase) and then released from the treatments for 4 h; Z, cells collected by mitotic shake-off technique after treated with 0.25 μM demecolcine for 12 h ($G_2$/M phases). (A) Representative distribution of cells with different DNA contents detected by flow cytometry in cells subjected to various conditions. (B) Whole-cell currents in response to 0, ±40 and ±80 mV steps from a holding potential 0 mV and activated by 47% hypotonic solution were recorded in cells collected from three independent groups ($n$ = 11, 14, and 10, in groups X, Y, and Z, respectively). The hypotonic-activated current was inhibited by 300 μM NPPB or 20 μM tamoxifen. (C) Comparison of volume-activated $Cl^-$ current at +80 and −80 mV among the three groups. (D) Cell distribution at different cell-cycle stages in the three groups. The data in the figure represent mean ± SE of 3–5 experiments in (A) and (D) and 10–14 cells in (B) and (C).**

the blocked cells progressed into S phase 4 h after release from the block. 90% of the cells harvested with the shake-off technique 12 h after incubation in the medium containing 0.25 μM demecolcine were in $G_2$/M phases.

### 3.3. Cell-cycle-dependent expression of volume-sensitive $Cl^-$ current

$Cl^-$ currents activated by 47% hypotonic solution in cells sampled at 48 h of incubation in the medium containing 0.2% fetal calf serum, with 82% of cells in $G_0/G_1$ phase (Fig. 2A, X), were large. These currents showed properties of outward rectification and negligible time-dependent inactivation. The mean value was 106.62 ± 6.95 pA/pF at +80 mV and −56.23 ± 5.25 pA/pF at −80 mV ($n$ = 12; Fig. 2B, X). These currents were inhibited by NPPB and tamoxifen, similar to those of unsynchronized cells.

In the cells arrested in S phase by the double chemical block technique (88% of cells in S phase as demonstrated by the flow cytometry; Fig. 2A, Y), the hypotonic-activated $Cl^-$ currents declined dramatically. The peak current (43.06 ± 6.02 pA/pF at +80 mV and −23.44 ± 4.23 pA/pF at −80 mV; $n$ = 18; Fig. 2B, Y) was much smaller than that of cells arrested at $G_0/G_1$ phase by serum starvation ($P < 0.01$), although the properties of the currents were similar. The current was sensitive to 300 μM NPPB and 20 μM tamoxifen.

For the cells synchronized in $G_2$/M phases (90% of cells in $G_2$/M phase; Fig. 2A, Z) by demecolcine and shake-off treatments, exposure to 47% hypotonic solution induced a $Cl^-$ current with properties similar to that of cells arrested in $G_0/G_1$ phases. The peak values of the current are 75.69 ± 6.95 pA/pF at +80 mV and −38.87 ± 7.52 pA/pF at −80 mV ($n$ = 10; Fig. 2B, Z). The current was smaller than that of $G_0/G_1$ (serum-starved) cells ($P < 0.01$), but larger than that of S cells released from the double chemical block ($P < 0.05$). The current was also sensitive to NPPB and tamoxifen.

Fig. 2C summarizes the expression of the $I_{Cl,vol}$ in the three groups of cells, $G_0/G_1$cells (serum-starved for 48 h, Fig. 2C, X), S cells (4 h after released from double chemical block, Fig. 2C, Y), and $G_2$/M cells (demecolcine block for 12 h and shake-off, Fig. 2C, Z). Fig. 2D shows the cell distribution at each stage of the cell cycle for the three groups using parallel flow cytometric analysis. The data indicate that the expression or activation of volume-activated $Cl^-$ channels was significantly modulated throughout the cell cycle. Channel activity was high in $G_0/G_1$ phase, down-regulated in S phase, but increased in $G_2$/M phase. There was no statistically significant difference in activation of volume-activated $Cl^-$ channels between cells synchronized at $G_2$/M phases by mitotic shake-off alone and those synchronized at $G_2$/M phases by demecolcine and mitotic shake-off treatments.

### 3.4. Cell-cycle-related changes in chemotactic migration of HeLa cells

As shown above, expression of $I_{Cl,vol}$ varied greatly as the cell cycle progressed. Previously in vitro studies in a variety of cell lines have shown that $I_{Cl,vol}$ is involved in cell migration [15,17,18]. The question remains, then, whether the migratory potential of HeLa cells shares this similar property with $I_{Cl,vol}$ during cell-cycle progression. To address this issue, migratory potential of HeLa cells was analyzed during the cell cycle using the transwell migration assay in synchronized cells.

$3 \times 10^5$ synchronized HeLa cells in $G_0/G_1$, S or $G_2$/M phases were added to the upper compartments of transwell chambers for chemotactic migration, and the rate of migration was calculated. As shown in Fig. 3A and B, pronounced changes in cell migration occurred as cells progressed from $G_0/G_1$ to $G_2$/M phases. The highest migratory rate was observed in $G_0/G_1$ phases, with approximately 25.57% cells migrated to the lower face of the membrane. The number of migrated cells in S phase decreased to 7.02%, the lowest rate of the three groups. In the $G_2$/M phases, however, an increase in migratory rate was observed with 11.42%. These data indicate that HeLa cells exhibit pronounced cell-cycle-related alterations in migration ability. Similar to the activities of volume-activated $Cl^-$ channels during cell-cycle progression, the potential of migration was high in $G_0/G_1$ phases, down-regulated in S phase, and again increased in $G_2$/M phases.

In order to investigate the relationship between $I_{Cl,vol}$ and cell migration further, we assessed the effects of $Cl^-$ channel blockers (NPPB and tamoxifen) on HeLa cell migration (Fig. 3C and D). Results show that the migration rate of $G_0/G_1$ cells treated with NPPB (300 μM), tamoxifen (20 μM) was significantly reduced, compared to that observed in the control cells ($G_0/G_1$ phase). NPPB and tamoxifen could also inhibit the migration of S and $G_2$/M cells (data not shown). These results show that reagents that inhibit $I_{Cl,vol}$ also slow cell migration.

### 3.5. Correlation between $I_{Cl,vol}$ and cell migration demonstrated by cell-cycle progression

As shown above, both the $I_{Cl,vol}$ and migration of HeLa cells were well regulated during cell-cycle progression. This relationship was further analyzed by comparing current level and migratory capability during cell-cycle progression. As shown in Fig. 4, cell migratory potential was plotted against the corresponding current (evoked at +80 mV step) of the $G_0/G_1$ group, S group, and $G_2$/M group. Fitting the data by linear regression resulted in a positive correlation between the two factors (migratory rate and current), with a linear correlation coefficient of $r$ = 0.96 ($P < 0.01$).

### 3.6. Effect of endogenous suppression of $I_{Cl,vol}$ on cell-cycle-dependent migration

The presented data thus far suggested that volume-activated chloride channels play an important role in cell-cycle-dependent migration of HeLa cells. ClC-3 has been suggested to be a component and/or regulator of volume-activated chloride channel activity. Inhibition of endogenous ClC-3 expression and function by antisense oligonucleotides against ClC-3 or an anti-ClC-3 antibody causes a decrease in $I_{Cl,vol}$ in bovine non-pigmented ciliary epithelial cells [24], smooth muscle cells [23,25], AGS cells [26], HeLa cells, and *Xenopus* oocytes [27]. We therefore investigated the effect of ClC-3 protein 'knock-down', using a ClC-3 antisense oligonucleotide, on cell-cycle-dependent migration of HeLa cells.

HeLa cells were transfected with fluorescein-labeled antisense and sense oligonucleotides for ClC-3. After 48 h,

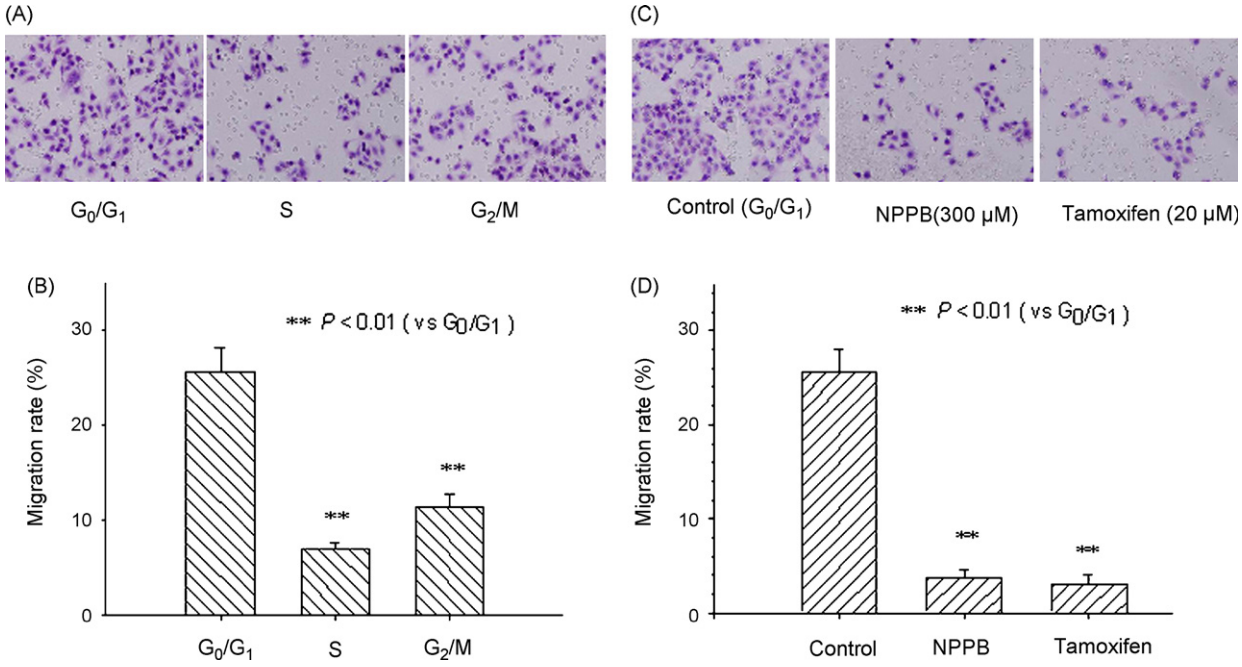


**Fig. 3 – Migratory potential of HeLa cells through the cell cycle. Synchronized cells were collected and seeded into upper compartments of transwell chambers for migration assays. The migration rate of cells synchronized in $G_0/G_1$, S or $G_2/M$ phases was measured. The number of migrated cells was captured by CCD camera imaging (100×) and assessed by MTT assay. (A) Photomicrographs of the bottom side of filters with migrated cells arrested in different cell-cycle stages, stained with the Hematoxylin and Eosin (HE) staining method. (C) Effects of chloride channel blockers NPPB and tamoxifen on migration of cells arrested in $G_0/G_1$ phases. Data are presented as mean ± SE of three independent experiments.**

fluorescence was observed in most cells showing that transfection efficiency was high. ClC-3 protein expression in cells harvested on day 2 was examined by Western blotting. Antisense oligonucleotides (20 μM) for ClC-3 significantly diminished ClC-3 protein expression to the level that was 15% of that observed in sense oligonucleotide-treated cells or in control non-transfected cells (Fig. 5A). Similarly, hypotonic-activated $Cl^-$ currents recorded from cells transfected with ClC-3 antisense oligonucleotides were quite different from those of control cells. In the antisense (20 μM) group, the hypotonic-induced currents were activated at a slower rate and the peak currents were reduced (Fig. 5B). The remained hypotonic-activated current could be inhibited by the chloride channel blocker tamoxifen (20 μM). Moreover, treating with

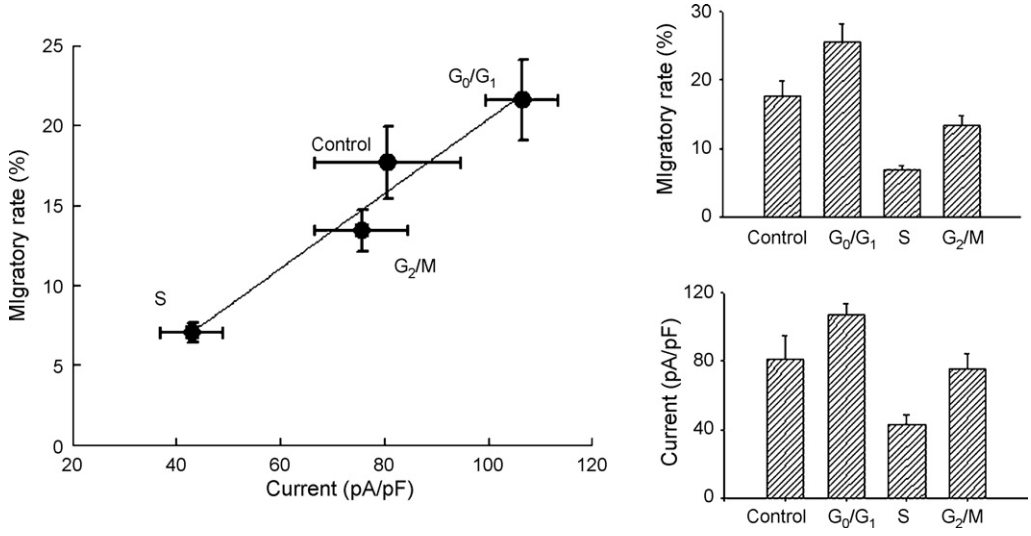


**Fig. 4 – Correlation between $I_{Cl,vol}$ and cell migration at different stages of the cell cycle. Plot of the mean value of migratory rate against that of the currents in each group indicated that the mean value of the migratory rate of cells is positively correlated to that of currents. A straight line was obtained by fitting the data with a linear regression equation, $y = y_0 + ax$.**

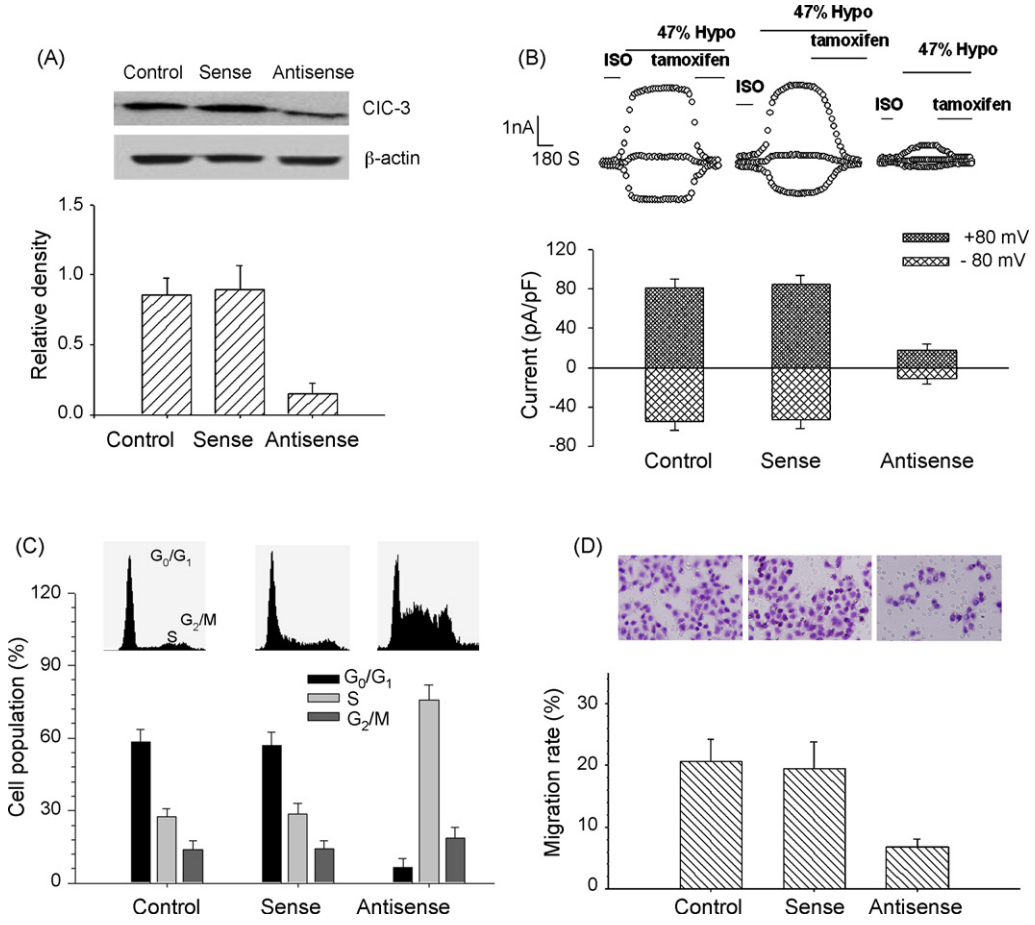


**Fig. 5 – Effects of endogenous inhibition of $I_{Cl,vol}$ expression on cell-cycle-dependent migration. After incubating with 20 μM ClC-3 antisense or sense oligonucleotides for 48 h, volume-activated chloride currents, cell-cycle distribution, and migration rate of transfected cells were measured. (A) Effects of ClC-3 antisense oligonucleotide transfection on ClC-3 protein expression in HeLa cells. (B) Inhibition of $I_{Cl,vol}$ by ClC-3 antisense oligonucleotides. Chloride channel blocker tamoxifen (20 μM) could inhibit the hypotonic-activated current in the three groups. (C) Effects of ClC-3 antisense transfection on cell-cycle distribution. (D) Effects of ClC-3 antisense transfection on HeLa cell migration, viewed with Hematoxylin and Eosin (HE) staining and detected with the MTT assay. Data in the figures are presented as means ± SE of 3–5 independent experiments.**

ClC-3 antisense oligonucleotides, which arrests cell-cycle progression at S phase, significantly decreased the rate of cell migration (Fig. 5C and D). The hypotonic-activated $Cl^-$ currents and migratory rate were not significantly different between cells treated with or without ClC-3 sense oligonucleotides. These results indicate that ClC-3 may mediate cell-cycle-dependent migration of HeLa cells by regulating volume-activated chloride channel activity, and also verify that $I_{Cl,vol}$ is involved in cell-cycle-dependent migration in HeLa cells.

## 4. Discussion

Recent studies have shown that migration of some mammalian cells is modulated in a cell-cycle-dependent manner. Several molecular candidates (p21 and p27) have been identified for their roles in regulating both cell cycle and cell migration. Although some controversy still exists regarding the relationship between volume-activated chloride current ($I_{Cl,vol}$) and cell cycle, $I_{Cl,vol}$ has been recognized to have important roles in modulating cell-cycle progression [9]. The findings from studies of Sontheimer and co-workers [15] and our previous research show that $I_{Cl,vol}$ is also involved in regulating tumor cell migration [18]. This suggests that volume-activated $Cl^-$ channels may play an important role in cell-cycle-dependent modulation of cell migration.

We first verified both expression and properties of $I_{Cl,vol}$ in HeLa cells. The recorded currents in this study are similar to those described previously in mammalian cells exposed to hypotonic solutions. The outward rectification, the observed reversal potential near the equilibrium potential for $Cl^-$, and the inhibition by the conventional $Cl^-$ channel blockers NPPB ($IC_{50}$ = 178.1 μM) and tamoxifen ($IC_{50}$ = 9.3 μM) are typical of $I_{Cl,vol}$ in many cell types, including HeLa cells. It has been shown that NPPB and tamoxifen inhibit $I_{Cl,vol}$ and cell proliferation in human nasopharyngeal carcinoma cells (tomoxifen, $IC_{50}$ = 16.9 μM for $I_{Cl,vol}$ and 15.6 μM for prolifera-

tion; NPPB, $IC_{50}$ = 96.5 μM for $I_{Cl,vol}$ and 98.0 μM for proliferation) [28] and in mouse liver cell (tomoxifen, $IC_{50}$ = 0.7 μM for $I_{Cl,vol}$ and 1.3 μM for proliferation; NPPB, $IC_{50}$ = 2.3 μM for $I_{Cl,vol}$ and 40 μM for proliferation) [29] and in canine colonic myocytes (tomoxifen, $IC_{50}$ = 0.6 μM for $I_{Cl,vol}$)[30]. It seems that the $IC_{50}$ of the two chloride channels blockers vary greatly in different cell types. Tamoxifen is also shown to inhibit the volume-sensitive current associated with the ClC-3 protein [31]. Our current results show that both the expression of $I_{Cl,vol}$ and cell migration in HeLa cells are cell-cycle-dependent. Moreover, the mean density of $I_{Cl,vol}$ was positively correlated to the rate of cell migration during cell-cycle progression. These results collectively indicate that volume-activated $Cl^-$ channels are involved in cell-cycle-dependent migratory behaviour of HeLa cells.

Endogenous inhibition of ClC-3 protein expression suppressed $I_{Cl,vol}$ [24,32]. To verify the role of volume-activated $Cl^-$ channels on cell-cycle-dependent migration, we investigated whether 'knock down' of ClC-3 protein expression affected $I_{Cl,vol}$, cell-cycle distribution and cell migration by using ClC-3 antisense oligonucleotides. Our results showed that decreasing ClC-3 protein expression by transfecting with antisense oligonucleotides diminished both $I_{Cl,vol}$ and cell migration. Moreover, consistent with our observation that rate of migration in S phase was the lowest among the three cell-cycle phases ($G_0/G_1$, S and $G_2$/M) in HeLa cells, inhibition of ClC-3 protein expression arrested the cell cycle at S phase. These data then provided compelling evidence that volume-activated $Cl^-$ channels play a critical role in cell-cycle-dependent migration of HeLa cells.

As stated above, tumor cell-cycle-dependent migration may be modulated by $I_{Cl,vol}$. How does this current affect cell-cycle-dependent migration? We speculate that $I_{Cl,vol}$ is involved in volume regulation during cell cycle and cell migration in HeLa cells, since volume regulation plays a critical role during both cell-cycle progression and migration. For example, in mammalian cells, cell volume continuously changes throughout the cell cycle [33]. Furthermore, an increase of cell volume coincides with entry of fibroblasts into S phase [34].Tumor cells must also undergo cell shape and volume changes as they navigate through the narrow, tortuous extracellular spaces [35]. Volume-activated chloride channels are of particular importance for regulatory volume decrease after cell swelling by mediating $Cl^-$ efflux. In fact, blockage of volume-activated chloride channels decreases RVD capacity [7,36]. Our previous work revealed that RVD plays an important role in migratory processes in tumor cells [20]. Similar to the cell-cycle-dependent change of $I_{Cl,vol}$, another previous work of ours showed that RVD capacity was actively regulated during the cell cycle, and that its capacity was highest in $G_1$ and lowest in S phase [37]. These imply that $I_{Cl,vol}$ may be involved in cell-cycle-dependent migration by regulating RVD.

Water outflow following ion efflux may be necessary for maintaining specific concentrations of critical elements for controlling cell-cycle progression. By regulating RVD, $I_{Cl,vol}$ may serve as an effective means of maintaining proper concentrations of cyclin/cyclin dependent kinase (CDK), endogenous CDK inhibitors (CDK inhibitors p15, p1, p18, p19, p20, p21, p27 and p57) and/or other important factors needed for regulating cell-cycle progression [9]. Blocking volume-activated chloride channels pharmacologically by $Cl^-$ channel blockers provoked cell-cycle arrest at $G_0/G_1$ phase and was also represented by p21 or p27 accumulation [38,39]. Several studies have revealed that p21 or p27 have CDK-independent cytoplasmic functions in cell migration, since up-regulation of either p21 or p27 inhibited cell migration [4–6,40]. These data indicate that blocking $I_{Cl,vol}$ may suppress cell migration by up-regulating p21 or/and p27 levels. This up-regulation may be an underlying mechanism that chloride channel blockers NPPB and tamoxifen almost completely inhibit cell migration of $G_0/G_1$ phase cells arrested by serum starvation. Therefore, $I_{Cl,vol}$ potentially plays a critical role in mediating high migratory potential in $G_0/G_1$ cells by regulating cell volume to maintain some molecular candidates, which is related to the regulation of both cell cycle and cell migration, on suitable concentration. However, how $I_{Cl,vol}$ regulates the different migration potentials related to S and $G_2$/M phase remains to be determined.

In conclusion, this study demonstrates that both $I_{Cl,vol}$ and cell migration are cell-cycle-dependent. We identified a positive correlation between the current and cell migration dependent on cell-cycle phases. Endogenous inhibition of $I_{Cl,vol}$ diminished cell migration and blocked cell-cycle progression. These results collectively indicate that the volume-activated $Cl^-$ channel plays important roles in cell-cycle-dependent migration in HeLa cells.

## Acknowledgements

This work was supported by the National Natural Science Foundation of China (30771106 and 30800435), Natural Science Foundation of Guangdong Province (07005974), Medical Science Research Grant of Guangdong Province (B2008086), and the Wellcome Trust (056909/299/Z).

## REFERENCES

[1] Boehm M, Nabel EG. Cell cycle and cell migration: new pieces to the puzzle. Circulation 2001;103:2879–81.
[2] Walmod PS, Hartmann-Petersen R, Prag S, Lepekhin EL, Ropke C, Berezin V, et al. Cell-cycle-dependent regulation of cell motility and determination of the role of Rac1. Exp Cell Res 2004;295:407–20.
[3] Ratner S, Jasti RK, Heppner GH. Motility of murine lymphocytes during transit through cell cycle Analysis by a new in vitro assay. J Immunol 1988;140:583–8.
[4] Denicourt C, Saenz CC, Datnow B, Cui XS, Dowdy SF. Relocalized p27Kip1 tumor suppressor functions as a cytoplasmic metastatic oncogene in melanoma. Cancer Res 2007;67:9238–43.
[5] Sun J, Marx SO, Chen HJ, Poon M, Marks AR, Rabbani LE. Role for p27(Kip1) in vascular smooth muscle cell migration. Circulation 2001;103:2967–72.
[6] Woods JM, Klosowska K, Spoden DJ, Stumbo NG, Paige DJ, Scatizzi JC, et al. A cell-cycle independent role for p21 in regulating synovial fibroblast migration in rheumatoid arthritis. Arthritis Res Ther 2006;8:R113.
[7] Sardini A, Amey JS, Weylandt KH, Nobles M, Valverde MA, Higgins CF. Cell volume regulation and swelling-activated

chloride channels. Biochim Biophys Acta 2003;1618:153–62.
[8] Stutzin A, Hoffmann EK. Swelling-activated ion channels: functional regulation in cell-swelling, proliferation and apoptosis. Acta physiol (Oxf Engl) 2006;187:27–42.
[9] Nilius B. Chloride channels go cell cycling. J Physiol 2001;532:581.
[10] Doroshenko P, Sabanov V, Doroshenko N. Cell cycle-related changes in regulatory volume decrease and volume-sensitive chloride conductance in mouse fibroblasts. J Cell Physiol 2001;187:65–72.
[11] Shen MR, Droogmans G, Eggermont J, Voets T, Ellory JC, Nilius B. Differential expression of volume-regulated anion channels during cell cycle progression of human cervical cancer cells. J Physiol (Lond) 2000;529(Pt 2):385–94.
[12] Klausen TK, Bergdahl A, Hougaard C, Christophersen P, Pedersen SF, Hoffmann EK. Cell cycle-dependent activity of the volume- and $Ca^{2+}$-activated anion currents in Ehrlich lettre ascites cells. J Cell Physiol 2007;210:831–42.
[13] Chen L, Wang L, Zhu L, Nie S, Zhang J, Zhong P, et al. Cell cycle-dependent expression of volume-activated chloride currents in nasopharyngeal carcinoma cells. Am J Physiol Cell Physiol 2002;283:C1313–2.
[14] Jakab M, Ritter M. Cell volume regulatory ion transport in the regulation of cell migration. Contrib Nephrol 2006;152:161–80.
[15] Ransom CB, O'Neal JT, Sontheimer H. Volume-activated chloride currents contribute to the resting conductance and invasive migration of human glioma cells. J Neurosci 2001;21:7674–83.
[16] Soroceanu L, Manning Jr TJ, Sontheimer H. Modulation of glioma cell migration and invasion using Cl(−) and K(+) ion channel blockers. J Neurosci 1999;19:5942–54.
[17] McFerrin MB, Sontheimer H. A role for ion channels in glioma cell invasion. Neuron Glia Biol 2006;2:39–49.
[18] Mao J, Wang L, Fan A, Wang J, Xu B, Jacob TJ, et al. Blockage of volume-activated chloride channels inhibits migration of nasopharyngeal carcinoma cells. Cell Physiol Biochem 2007;19:249–58.
[19] Mao JW, Wang LW, Sun XR, Zhu LY, Li P, Zhong P, et al. Volume-activated $Cl^-$ current in migrated nasopharyngeal carcinoma cells. Sheng Li Xue Bao 2004;56:525–30.
[20] Mao JW, Wang LW, Jacob T, Sun XR, Li H, Zhu LY, et al. Involvement of regulatory volume decrease in the migration of nasopharyngeal carcinoma cells. Cell Res 2005;15:371–8.
[21] Doyle AGJ, Newell DG. Cell and tissue culture: laboratory procedures. Chichester, UK: Wiley; 1993.
[22] Gaffney EV. The accumulation and selective detachment of mitotic cells. Methods Cell Biol 1975;9:71–84.
[23] Wang GX, Hatton WJ, Wang GL, Zhong J, Yamboliev I, Duan D, et al. Functional effects of novel anti-ClC-3 antibodies on native volume-sensitive osmolyte and anion channels in cardiac and smooth muscle cells. Am J Physiol Heart Circ Physiol 2003;285:H1453–6.
[24] Wang L, Chen L, Jacob TJ. The role of ClC-3 in volume-activated chloride currents and volume regulation in bovine epithelial cells demonstrated by antisense inhibition. J Physiol (Lond) 2000;524(Pt 1):63–75.
[25] Duan D, Zhong J, Hermoso M, Satterwhite CM, Rossow CF, Hatton WJ, et al. Functional inhibition of native volume-sensitive outwardly rectifying anion channels in muscle cells and *Xenopus* oocytes by anti-ClC-3 antibody. J Physiol (Lond) 2001;531:437–44.
[26] Jin NG, Kim JK, Yang DK, Cho SJ, Kim JM, Koh EJ, et al. Fundamental role of ClC-3 in volume-sensitive $Cl^-$ channel function and cell volume regulation in AGS cells. Am J Physiol Gastrointest Liver Physiol 2003;285:G938–48.
[27] Hermoso M, Satterwhite CM, Andrade YN, Hidalgo J, Wilson SM, Horowitz B, et al. ClC-3 is a fundamental molecular component of volume-sensitive outwardly rectifying $Cl^-$ channels and volume regulation in HeLa cells and *Xenopus laevis* oocytes. J Biol Chem 2002;277:40066–74.
[28] Chen LX, Zhu LY, Jacob TJ, Wang LW. Roles of volume-activated $Cl^-$ currents and regulatory volume decrease in the cell cycle and proliferation in nasopharyngeal carcinoma cells. Cell Prolif 2007;40:253–67.
[29] Wondergem R, Gong W, Monen SH, Dooley SN, Gonce JL, Conner TD, et al. Blocking swelling-activated chloride current inhibits mouse liver cell proliferation. J Physiol (Lond) 2001;532:661–72.
[30] Dick GM, Kong ID, Sanders KM. Effects of anion channel antagonists in canine colonic myocytes: comparative pharmacology of $Cl^-$ $Ca^{2+}$ and $K^+$ currents. Br J Pharmacol 1999;127:1819–31.
[31] Duan D, Winter C, Cowley S, Hume JR, Horowitz B. Molecular identification of a volume-regulated chloride channel. Nature 1997;390:417–21.
[32] Mao J, Chen L, Xu B, Wang L, Li H, Guo J, et al. Suppression of ClC-3 channel expression reduces migration of nasopharyngeal carcinoma cells. Biochem Pharmacol 2008;75:1706–16.
[33] Bussolati O, Uggeri J, Belletti S, Dall'Asta V, Gazzola GC. The stimulation of Na, K, Cl cotransport and of system A for neutral amino acid transport is a mechanism for cell volume increase during the cell cycle. FASEB J 1996;10:920–6.
[34] Pendergrass WR, Angello JC, Kirschner MD, Norwood TH. The relationship between the rate of entry into S phase, concentration of DNA polymerase alpha, and cell volume in human diploid fibroblast-like monokaryon cells. Exp Cell Res 1991;192:418–25.
[35] Schwab A. Function and spatial distribution of ion channels and transporters in cell migration. Am J Physiol Renal Physiol 2001;280:F739–47.
[36] Okada Y. Cell volume-sensitive chloride channels. Contrib Nephrol 1998;123:21–33.
[37] Wang L, Chen L, Zhu L, Rawle M, Nie S, Zhang J, et al. Regulatory volume decrease is actively modulated during the cell cycle. J Cell Physiol 2002;193:110–9.
[38] Jiang B, Hattori N, Liu B, Nakayama Y, Kitagawa K, Inagaki C. Suppression of cell proliferation with induction of p21 by Cl(−) channel blockers in human leukemic cells. Eur J Pharmacol 2004;488:27–34.
[39] Renaudo A, L'Hoste S, Guizouarn H, Borgese F, Soriani O. Cancer cell cycle modulated by a functional coupling between sigma-1 receptors and $Cl^-$ channels. J Biol Chem 2007;282:2259–67.
[40] Fukui R, Shibata N, Kohbayashi E, Amakawa M, Furutama D, Hoshiga M, et al. Inhibition of smooth muscle cell migration by the p21 cyclin-dependent kinase inhibitor (Cip1). Atherosclerosis 1997;132:53–9.